

Assessment of the Safety Factor Evolution of the Shotcrete Lining for Different Curing Ages

Original

Assessment of the Safety Factor Evolution of the Shotcrete Lining for Different Curing Ages / Oreste, P., Spagnoli, G., Luna Ramos, C.A., Hedayat, A.. - In: GEOTECHNICAL AND GEOLOGICAL ENGINEERING. - ISSN 0960-3182. - STAMPA. - 37:6(2019), pp. 5555-5563. [10.1007/s10706-019-00990-2]

Availability:

This version is available at: 11583/2787828 since: 2020-01-31T12:46:13Z

Publisher:

Springer International Publishing

Published

DOI:10.1007/s10706-019-00990-2

Terms of use:

This article is made available under terms and conditions as specified in the corresponding bibliographic description in the repository

Publisher copyright

(Article begins on next page)

1 **Assessment of the safety factor evolution of the shotcrete lining for different curing**
2 **ages**

3 Pierpaolo Oreste¹, Giovanni Spagnoli^{2*}, Cesar Alejandro Luna Ramos³, Ahmadreza
4 Hedayat⁴

5 ¹ Full Professor, Department of Environmental, Land and Infrastructural Engineering,
6 Politecnico di Torino, Corso Duca Degli Abruzzi 24, 10129 Torino, Italy,
7 pierpaolo.oreste@polito.it, ORCID: 0000-0001-8227-9807

8 ² Global Project and Technology Manager Underground Construction, BASF Construction
9 Solutions GmbH, Dr.-Albert-Frank-Straße 32, 83308 Trostberg, Germany, *
10 giovanni.spagnoli@basf.com, ORCID: 0000-0002-1866-4345

11 ³ Professor, Faculty of Engineering, Universidad Mariana, Faculty of Engineering,
12 Universidad Mariana, Calle 18 No. 34-104, Pasto, Colombia, celuna@umariana.edu.co.
13 Former MSc student at Department of Environmental, Land and Infrastructural Engineering,
14 Politecnico di Torino, Corso Duca Degli Abruzzi 24, 10129 Torino, Italy

15 ⁴ Assistant Professor, Department of Civil and Environmental Engineering, Colorado School
16 of Mines, 1500 Illinois Street, Golden, CO 80401, USA, hedayat@mines.edu, ORCID: 0000-
17 0002-7143-7272

18 **Abstract**

19 The behavior of the shotcrete linings during the tunnel construction is complex due to the
20 variability of its mechanical characteristics during the curing time. During the curing time, the
21 lining is loaded along with the excavation face of the tunnel advance. A new calculation
22 procedure involving two analytical methods, i.e. the convergence-confinement method and
23 hyperstatic reaction method have been developed. By means of these two methods, it is
24 possible to assess the evolution of the stress state in the lining, and therefore, also of the
25 safety factor with respect to the failure in compression of the shotcrete. Due to the analysis of

26 the safety factor evolution over time, it is possible to correctly design the lining, to choose the
27 type of sprayed concrete and to define the maximum admissible advance rate of the
28 excavation face, in order not to critically load the lining. In the following paper, after having
29 shown the definition of the safety factor, a parametric analysis is performed, in order to
30 investigate the evolution of the safety factor of the lining for two different rock types, three
31 different shotcrete types and two tunnel advance rates have been considered.

32 **Key words:** sprayed concrete; convergence-confinement method; hyperstatic reaction
33 method; accelerator; safety factor; curing age.

34 **No. of Figs: 5**

35

36 **Nomenclature**

37	b	Depth of the lining considered, equal to 1m in the two-dimensional problem
38		taken into consideration
39	c_{rm} peak	Peak cohesion of the rock mass
40	c_{rm} res	Residual cohesion of the rock mass
41	E_{rm}	Elastic modulus of the rock mass
42	E_{SC}	Elastic modulus of the sprayed concrete with varying time t (in hours) after the
43		lining installation in the studied section
44	$E_{SC,\infty}$	Asymptotic values of the elastic modulus of the sprayed concrete reached for
45		high time values
46	FS	Safety factor
47	$M_{i,j}$	Bending moment in the i -th node, at the load step j -th
48	$N_{i,j}$	Normal force in the i -th node, at the load step j -th
49	t	Lining thickness
50	ν	Poisson ratio
51	α	Exponent of the exponential equation, which characterizes the curing rate, i.e.
52		the evolution of mechanical parameters (elastic modulus and uniaxial
53		compressive strength) of SC over time
54	ϕ_{rm} peak	Peak friction angle of the rock mass
55	ϕ_{rm} res	Residual friction angle of the rock mass
56	ψ	Dilatancy

57	$\sigma_{n,max,i,j}$	Maximum normal stress acting inside the sprayed concrete in correspondence
58		of a node
59	σ_{SC}	Unconfined compressive strength of the sprayed concrete with varying time t
60		(in hours) after the lining installation in the studied section
61	$\sigma_{SC,\infty}$	Asymptotic values of the Unconfined compressive strength of the sprayed
62		concrete, reached for high t values
63		

64 **Introduction**

65 DIN 18551 (2014) defines sprayed concrete (or shotcrete), abbreviated here as SC, as
66 *“concrete which is conveyed under pressure through a pneumatic hose or pipe and projected*
67 *into place at high velocity, with simultaneous compaction”* (see Fig. 1).



68

69 **Fig. 1 Sprayed concrete trials in a job site.**

70 Because SC takes care of stability problems in tunnels and other underground constructions
71 (Melbye 1994) immediately after the installation, early-age strength and time-dependent
72 behavior of SC both in soil and rock ground conditions is relevant (Thomas 2009);
73 furthermore the time dependent behavior is frequently more important than its ultimate
74 strength, because the advance rate (AR) of the tunnel face is strongly influenced by the rate
75 of development of the SC early-age strength (Mohajerani et al. 2015). The time dependent
76 behavior of shotcrete needs to be considered for realistic ground-support interactions and
77 several constitutive models for shotcrete as a function of curing time currently exist in the

78 literature. Bryne (2014) conducted extensive compressive strength and Young's modulus
79 evaluation of shotcrete with time and developed in-situ test techniques for determination of
80 sprayed shotcrete bond strength. Several studies employed a constitutive law for time
81 dependent stiffness and strength of the shotcrete (e.g., Pan and Huang, 1994; Graziani et al.
82 2005; Schütz 2010).

83 The early-age strength of SC is frequently more important than its ultimate strength. The
84 advance speed of tunnel operations is strongly influenced by the rate of development of
85 early-age strength, since it determines, both in soft ground and weak rock, when excavation
86 heading can proceed. As a matter of fact, re-entry is mainly driven by the tunnel drive
87 progression to ensure the safety of personnel to continue development (Mohajerani et al.
88 2015). Re-entry times range from 2 to 4 h, where the Unconfined Compressive Strength
89 (UCS) reaches 1MPa (Clements 2004; Concrete Institute of Australia 2010), however, this
90 value is not standardized and it can be also lower, if safety is ensured (see Rispin et al.
91 2009). Iwaki et al. (2001) empirically determined that an UCS of 0.5–1MPa should be an
92 adequate strength for SC to protect against rock-fall, although the safe re-entry times, based
93 on strength measurements, is still determined on project basis (Mohajerani et al. 2015).

94 Therefore, additives are used to accelerate the hydration reaction (Thomas 2009).
95 Accelerated SC has a shorter final setting time and higher early-age compressive strength
96 compared with conventional concrete (Prudencio 1998) and it can be used in tunneling
97 successfully. The use of accelerators allows for good adhesiveness, lower amount of
98 rebounding, good spraying, and accelerated strength gain, as desired properties for
99 shotcrete (Qiu et al. 2017).

100 Nowadays, accelerators for SC are normally based on combinations of aluminium salts
101 (sulphates, hydroxides and hydroxysulphates) (DiNoia and Sandberg 2004). Aluminum
102 sulfate is the most common type of accelerator being used (). In wet mix, the accelerator is
103 added in liquid form at the nozzle during spraying. For dry mix, the accelerator can also be
104 added as a fixed dosage in powder form when using pre-bagged mixes (Thomas 2009).

105 Accelerators considerably improve the setting which should be ≤ 60 min (prEN 934-5 2003)
106 for SC applications, against the 6 to 7 h normally needed in Ordinary Portland Cement (De
107 Belie et al. 2005).

108 In numerical modeling the curing of the cement in the SC lining is very important, as the
109 mechanical improvements (compressive strength and elastic modulus) change the behavior
110 of the linings. These transient conditions are a critical situation for the stability of the support
111 structure during the tunnel construction, influencing the final equilibrium of the lining (Oreste
112 2003).

113 There are several methods to numerically model sprayed concrete structures. Elastic method
114 with a constant stiffness (e.g. Pöttler, 1990; Feenstra and de Borst 1993; Rokhar and
115 Zachow, 1997), linear elastic material behavior models (for instance using the Hypothetical
116 Modulus of Elasticity, HME) (e.g. Pöttler 1990), non-linear models considering strain
117 hardening (e.g. Kotsovos and Newman 1978; Aydan et al. 1992; Moussa, 1993; Neville
118 1995), elastic perfectly plastic constitutive models (e.g. Chen 1982; Hellmich et al. 1999;
119 Thomas 2009), plastic models (e.g. Meschke 1996; Schütz et al. 2011; Schädlich and
120 Schweiger 2014). Nuener et al. (2017) conducted a study and evaluated the influence of
121 different constitutive models for shotcrete on the stresses and displacements in shotcrete
122 shells in deep tunnels and reported different amount of creep and shrinkage in concrete.

123 The following paper considers the Converge Confinement Method (CCM) and the
124 Hyperstatic Reaction Method (HRM) to jointly study in the detail the behavior of the tunnel
125 support under external loads with different elastic modulus values of SC during the curing
126 phase. The final stress state of the lining is the result of a complex loading mechanism due to
127 the excavation face advance (while the SC hardens) and the corresponding variations in its
128 mechanical characteristics (Oreste 2003). CCM generally requires a mean stiffness of the
129 SC lining to obtain the support reaction line (Oreste 2003). In this research, the reaction line
130 of the SC lining is considered as variable (curved and not linear), in order to simulate the
131 curing effect of the SC during the loading phase of the lining. The variation over time of the

132 elastic modulus of SC is considered by modifying the stiffness of the support and therefore
133 the slope of the reaction line of the SC lining. Time is indirectly considered by associating the
134 different positions of the excavation face with respect to the studied section reached in the
135 time, considering the evolution of the setting time of the SC and therefore to its elastic
136 modulus.

137 CCM was useful to evaluate the magnitude of the various loading steps developing over time
138 during the face excavation. In HRM method, the interaction between ground and support is
139 represented by Winkler type springs. This method allows for determining the displacement of
140 the lining and the developed bending moments and forces in order to design it (Oreste 2007;
141 Do et al. 2014a). In the specific case, different loading steps obtained with the CCM, have
142 been applied at the HRM model considering for each of these the effective stiffness value
143 reached by the SC and hence by the support structure.

144 From the calculation results it is possible to determine the final mechanical conditions of the
145 SC lining, that is, when the excavation face is far away from the tunnel section analyzed.
146 Besides, it is also possible to determine, what occurs in the transition phases (for limited
147 timings), when the applied load on the lining is not yet the final one. In this case the SC still
148 has a strength and an elastic modulus lower than the final asymptotic values. From the
149 comparison between the strength reached over the time of the SC and the final stress state
150 in the lining, it is possible to evaluate the safety factor (FS) in the support structure. FS can
151 be plotted as function of time after the installation of the lining in the evaluated section.
152 These graphs are interesting as they allow to evaluate critical situations (minimum FS
153 values) in the transition phases, when SC has not fully cured yet. In this research, after a
154 brief description of the two methods employed for the calculation, a parametric analysis is
155 conducted. The analysis considers three different SC types (with different curing ages) and
156 two difference advancement rates (ARs) of the excavation face (with consequent different
157 load stages of the lining). The analysis allows to assess the evolution of FS over time and to
158 estimate critical phases during the transition load stages of the lining during the SC curing.

159 The combined analysis of the two calculation methods provided a detailed evaluation of the
160 stress state of the support, which can consider both the effect of the mechanical
161 characteristics of the employed SC (with the evolving curve of strength and stiffness with the
162 time) and the advance rate of the excavation face.

163 **Analytical methods**

164 The analysis of the behavior of the SC linings, during the setting phase and, therefore, during
165 the construction of the tunnel is quite complex with the traditional numerical methods. In fact,
166 it is necessary to update the mechanical characteristics of the SC at each calculation step,
167 linking them with the time after the installation of the lining in the investigated section and the
168 position of the excavation face with respect to the studied section. The knowledge of the
169 evolution of the mechanical parameters of the SC over time, in fact requires to define the
170 elastic modulus of the SC at each calculation step. The position of the excavation face and,
171 therefore, the progress of the excavation work, influences the loading mode of the lining in
172 the studied section. In the three-dimensional numerical methods this happens automatically,
173 since the construction of the tunnel is simulated according to the exact sequence of the
174 excavation steps and the realization of the supports. In two-dimensional numerical methods,
175 however, the position of the face is considered by inserting on the perimeter of the gallery an
176 appropriate fictitious internal pressure, which is gradually decreasing as the excavation face
177 advances.

178 Given the difficulties of the traditional numerical modeling to represent the correct evolution
179 of the SC during the loading phase of the support, a new calculation procedure was
180 developed (see Oreste et al. 2018a; 2018b) based on two analytical methods, very
181 widespread in the field of tunnels and easy to use: the convergence-confinement method
182 (CCM), see Oreste, (2009; 2014); Fahimifar and Hedayat (2008; 2010) and Spagnoli et al.
183 (2016; 2017) and the hyperstatic reaction method (HRM), see Oreste (2007) and Do et al.
184 (2014a; 2014b). The CCM allows to evaluate with a certain precision the various load steps
185 acting on the lining, and, for each of them, to define the value of the elastic modulus reached

186 by the SC. This is done by determining the convergence-confinement curves of the tunnel
187 and, subsequently, the reaction line of the lining in SC. The latter is determined by points,
188 through the definition of different steps, based on the AR of the excavation face and the
189 evolution of the elastic modulus of the SC over time.

190 The detailed analysis of the stress state in the lining is then assigned to the HRM. This
191 analytical method uses a numerical solution to finite elements (FEM). The lining is simulated
192 through a succession of one-dimensional elements (beam elements) connected in series
193 through the nodes. On the same nodes of the numerical model, springs (normal and
194 transversal) representing the interaction between the lining and the rock wall of the tunnel
195 are connected. The load steps obtained from the analysis with the CCM are applied to the
196 model and for each of them we proceed to update the elastic modulus of the SC in the one-
197 dimensional elements. The results of the calculation for each load step allow to obtain the
198 progress of the bending moments, of the normal forces and of the shear forces, as well as of
199 the displacements, in the lining, along its whole length. At each load step, the results of that
200 step are then added to the results achieved by all the previous loading steps.

201 If the bending moment M and the normal force N acting at each node of the lining (i) reached
202 at the load step j are known, it is possible to determine the maximum normal stress $\sigma_{n,max,i,j}$,
203 acting inside the SC in correspondence of that node:

$$204 \quad \sigma_{n,max,i,j} = \frac{M_{i,j}}{\left(\frac{b \cdot s^2}{6}\right)} + \frac{N_{i,j}}{(b \cdot t)} \quad (1)$$

205 where:

206 b : width of the lining considered, equal to 1m in the two-dimensional problem taken into
207 consideration;

208 $M_{i,j}$: bending moment in the i -th node, at the load step j -th;

209 $N_{i,j}$: normal force in the i -th node, at the load step j -th;

210 t : lining thickness.

211 Among all the values of $\sigma_{n,max,i,j}$ obtained in the various nodes, the maximum value between
212 the normal stress acting in the various nodes of the model is then identified, which is
213 associated with the j-th load step:

$$214 \quad \sigma_{n,max,j} = \max(\sigma_{n,max,i,j}) \quad (2)$$

215 The local safety factor FS_j of the lining on the j-th load step is then evaluated according to the
216 following equation:

$$217 \quad FS_j = \frac{\sigma_{c,j}}{\sigma_{n,max,j}} \quad (3)$$

218 where:

219 $\sigma_{c,j}$: the strength reached by the SC at the j-th load step, knowing the time associated with
220 each load step.

221 FS calculated above is a local FS, which allows to verify the possible presence of local failure
222 over the SC lining. Local failures do not jeopardize the overall stability of the lining, however
223 they can lead to cracks in the support which may turn out in a global failure. The design of
224 the support must therefore consider local FS values to avoid global failures of the structure.

225 Since the time t following the realization of the lining in the studied section and the position of
226 the excavation face (in particular the distance reached by the front with respect to the studied
227 section) is associated with each loading step, the calculation procedure allows to plot FS of
228 the SC lining depending on the time or on the distance reached by the excavation face with
229 respect to the studied section. These trends make possible to quickly check whether there is
230 a critical situation in the transient conditions of the lining, or if the minimum FS of the lining is
231 reached in the long term (as an asymptotic value as discussed above). The procedure is able
232 to compare the progress of FS for different types of SC (with and without accelerators) or
233 also for different AR of the excavation face, so that the right type of SC can be chosen to
234 ensure stability both during the construction of the work and in the long term, when the work
235 has been completed.

236 **Results and discussion**

237 To analyze the evolution of FS of the SC lining with the calculation procedure developed, the
 238 case of a circular tunnel with 7m radius excavated in two different rock types with RMR = 60
 239 (fair), and RMR = 80 (good), as suggested by Bieniawski (1989), was analyzed. The
 240 mechanical characteristics of the two rock masses considered are shown in Tables 1 and 2.

241 The lithostatic stress state of the rock mass p_0 was assumed to be equal to 7MPa,
 242 corresponding to a depth of the tunnel from the ground surface equal to about 300m.

Rock Mass Parameters	Units	Value
Elastic modulus (E_{rm})	[MPa]	21,170
Poisson ratio (ν)	[-]	0.30
Peak cohesion (c_{rm} peak)	[MPa]	1.50
Residual cohesion (c_{rm} res)	[MPa]	1.50
Peak friction angle (ϕ_{rm} peak)	[°]	33
Residual friction angle (ϕ_{rm} res)	[°]	33
Dilatancy (ψ)	[°]	16

243 **Table 1. Mechanical characteristics of the rocky type 1 (RMR = 60), considered in the**
 244 **studied example.**

Rock Mass Parameters	Units	Value
Elastic modulus (E_{rm})	[MPa]	57,500
Poisson ratio (ν)	[-]	0.30
Peak cohesion (c_{rm} peak)	[MPa]	3.75
Residual cohesion (c_{rm} res)	[MPa]	3.75
Peak friction angle (ϕ_{rm} peak)	[°]	42
Residual friction angle (ϕ_{rm} res)	[°]	42
Dilatancy (ψ)	[°]	16

245 **Table 2. Mechanical characteristics of the rocky type 2 (RMR = 80), considered in the**
 246 **studied example.**

247 Pöttler (1990) introduced the coefficient α by suggesting a method to represent the variation
 248 of the elastic modulus over the time.

$$E_{,t} = E_{,0} \cdot (1 - e^{-\alpha \cdot t}) \quad (4)$$

249 where:

- 250 • $E_{,t}$ is the SC elastic modulus at the time t ;
- 251 • $E_{,0}$ is the value of the asymptotic elastic modulus of the SC, for $t = \infty$;

252 • α is the exponent of the exponential equation, which characterizes the curing rate,
253 i.e. the evolution of mechanical parameters over time (Oreste 2003).

254 The ratio between the elastic modulus and UCS is considered constant over time. This is given
255 by the equation of Chang (1993):

$$\sigma_{c,t} = \left(\frac{E_{c,t}}{3.86} \right)^{1/0.6} \quad (5)$$

256 Where:

257 $\sigma_{c,t}$ is the UCS for the SC at the time t .

258 Three different SC types have been considered:

259 a) a SC with fast curing rate, (SC_A) ($\alpha=0.09$);

260 b) a SC with medium curing rate, (SC_B) ($\alpha=0.05$);

261 c) a SC with low curing rate, (SC_C) ($\alpha=0.03$).

262 For all three SC types, a final value of elastic modulus ($E_{SC,\infty}=28\text{GPa}$) and unconfined
263 compressive strength, UCS, ($\sigma_{SC,\infty}= 27\text{MPa}$) was arbitrary assumed. The evolution over time
264 of the elastic modulus and UCS was assumed to be identical, that means with the same
265 value of α (Weber 1979; Pöttler 1990; Oreste 2003):

$$266 \quad E_{SC} = E_{SC,\infty} \cdot (1 - e^{-\alpha t}) \quad (6)$$

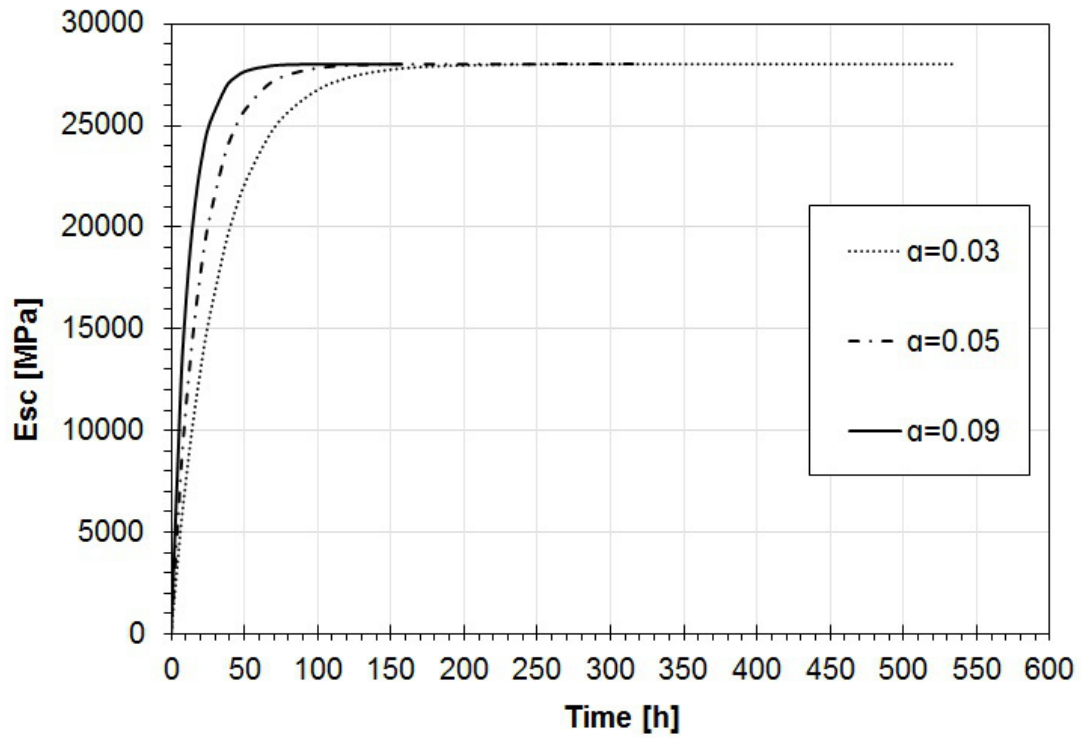
$$267 \quad \sigma_{SC} = \sigma_{SC,\infty} \cdot (1 - e^{-\alpha t}) \quad (7)$$

268 Where:

269 E_{SC} and σ_{SC} : Elastic modulus and UCS of the SC with varying time t (in hours) after the lining
270 installation in the studied section;

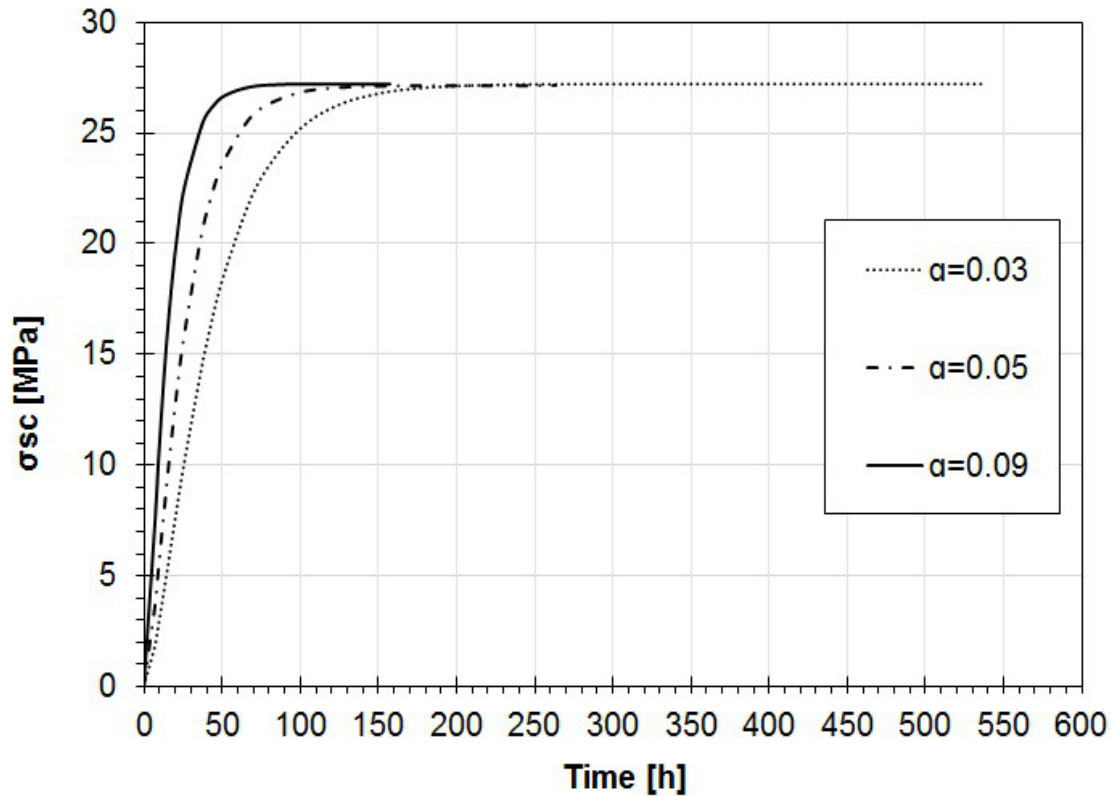
271 $E_{SC,\infty}$ and $\sigma_{SC,\infty}$: Asymptotic values of the elastic modulus and UCS of the SC, reached for
272 high t values;

273 The trend over time of the elastic modulus and UCS of the SC for the three types considered
274 is shown in Figures 2 and 3.



275

276 **Fig. 2 Trend of the elastic modulus over time for the three SC types considered in the**
 277 **numerical example: SC_A: SC with fast curing rate ($\alpha=0.09$); SC_B: SC with medium**
 278 **curing rate ($\alpha=0.05$) and SC_C: SC with low curing rate ($\alpha=0.03$).**

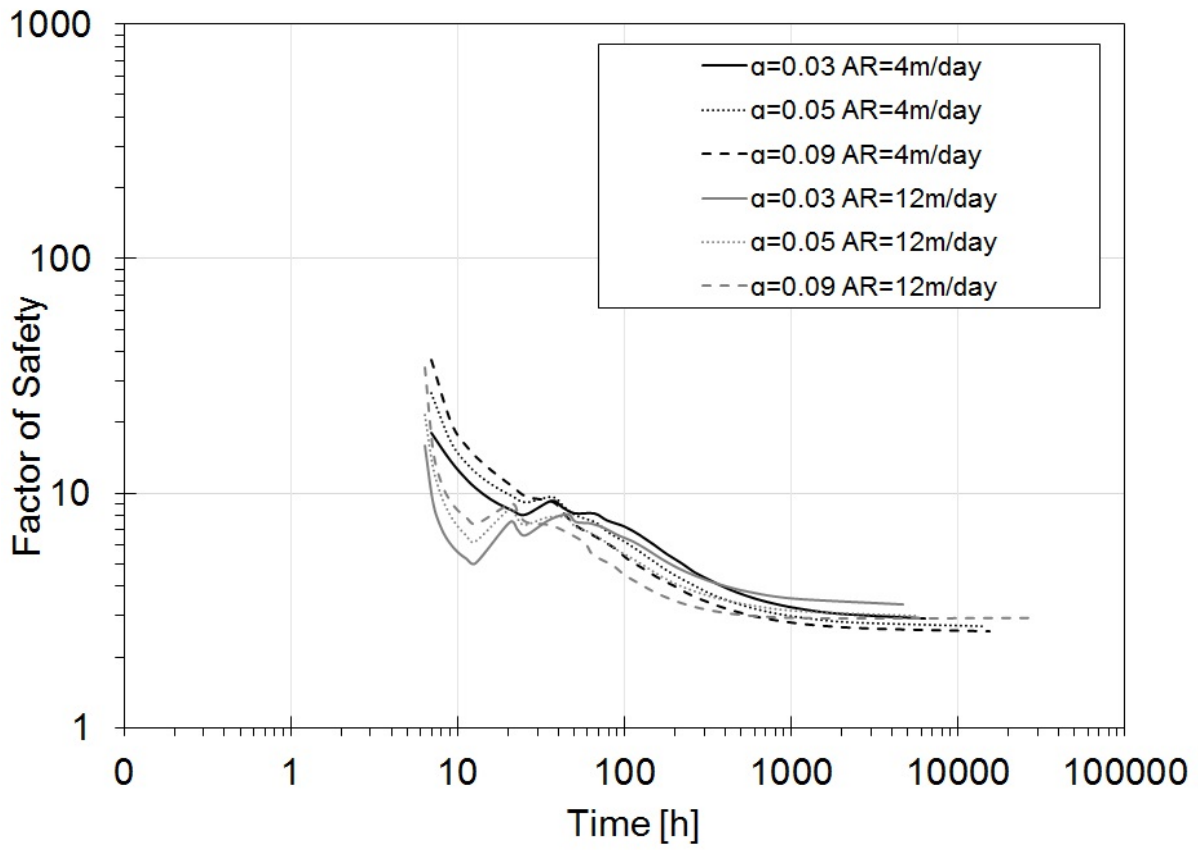


279

280 **Fig. 3 Trend of UCS over time for the three SC types considered in the numerical**
 281 **example: SC_A: SC with fast curing rate ($\alpha=0.09$); SC_B: SC with medium curing rate**
 282 **($\alpha=0.05$) and SC_C: SC with low curing rate ($\alpha=0.03$).**

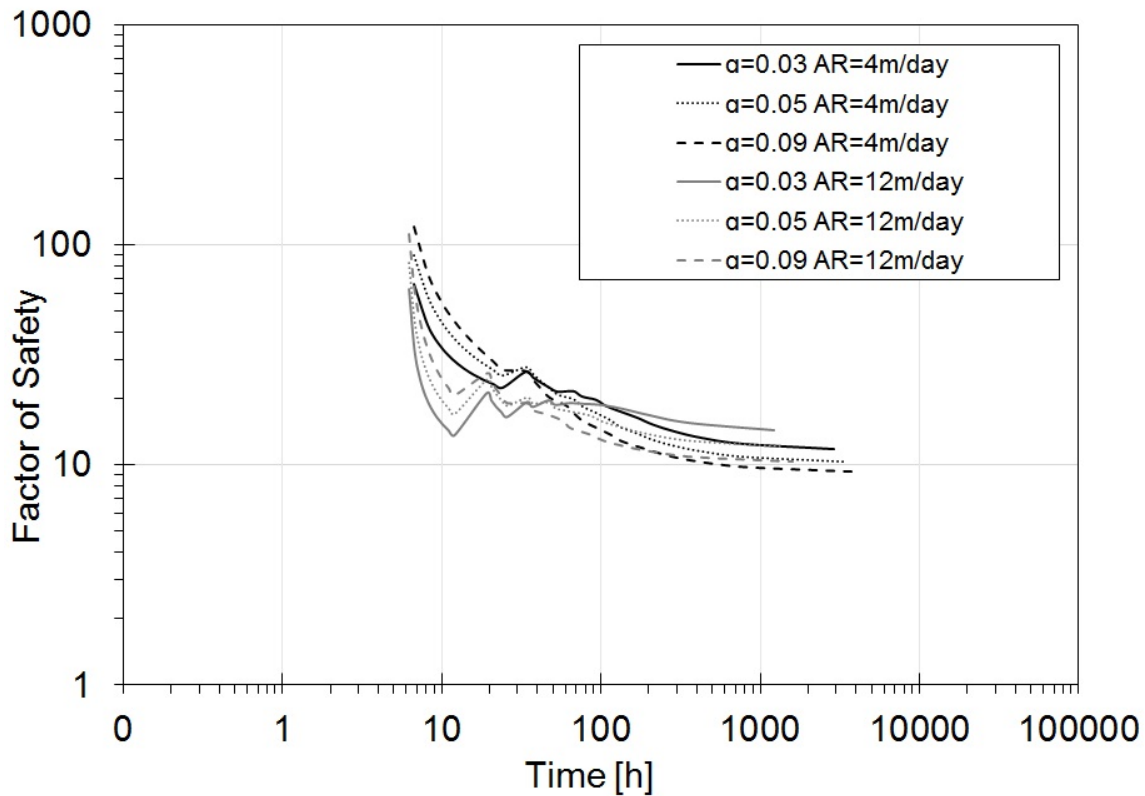
283 Furthermore, two different ARs of the excavation face have been arbitrary considered:
 284 4m/day and 12m/day. The two different rates produce different speed of the load application
 285 to the lining, with consequences on the stress state induced in the SC.

286 The calculation by first the CCM and then with the HRM allowed to determine the values of
 287 the bending moments M and of the normal forces N along the development of the entire
 288 lining. From the values of M and N the maximum normal stresses in the SC were obtained
 289 for each load step and, then, FS with respect to the compression failure. Below the results in
 290 terms of FS for the two rock masses, the three types of SC and the two ARs studied are
 291 shown. FS are diagrammed according to the time following the lining installation in the
 292 studied section.



293

294 **Fig. 4 Rock type 1: Evaluation of FS over time for the three SC types (SC_A ($\alpha=0.09$), SC_B**
 295 **($\alpha=0.05$) and SC_c ($\alpha=0.03$)) and two advance rates.**



296

297 **Fig. 5 Rock type 2: Evaluation of FS over time for the three SC types (SC_A ($\alpha=0.09$), SC_B**
 298 **($\alpha=0.05$) and SC_c ($\alpha=0.03$)) and two advance rates.**

299 The analysis of the results shows above all that the same SC lining has lower **local** FS for
 300 the rock type 1, the poorest one among the two considered (Fig. 4). In addition, we note the
 301 influence of the type of SC and the AR on FS in both rock masses, mainly for the rock mass
 302 with higher geomechanical quality (type 2), see Fig. 5. In general, the long-term FS is lower
 303 for fast-curing SCs and lower ARs. AR results to have a negligible effect in the poorest rock
 304 mass.

305 In the transitory conditions, however, there is the presence of relative minima, which may be
 306 significant, above all for high ARs and slow curing rate. This phenomenon is more
 307 pronounced in the rock mass of superior geomechanical quality. Among the 12 cases
 308 studied, just for the case of rock masses type 2, $v = 12\text{m/day}$ and type SC_c (with α coefficient
 309 of 0.03) a minimum value of FS in the transient condition is noticed (after a few hours

310 compared to the lining installation) lower than the final asymptotic value, representative of
311 the long-term condition.

312 This circumstance is particularly significant and requires a lot of attention by the tunnel
313 engineers. It can indicate the presence of critical aspects regarding the stability of the lining
314 in a transitory condition, when the SC has not yet completed the curing phase during the
315 tunnel construction.

316 **Conclusions**

317 A new calculation procedure has been used which is able to study in detail the mechanical
318 behavior of the lining during the tunnel construction. This procedure is based on two
319 analytical methods used in succession: the convergence-confinement method (CCM) and the
320 hyperstatic reaction method (HRM). The first one allows evaluating the load steps applied to
321 the lining and, for each one, the value of the elastic modulus reached by the SC. The second
322 helps to calculate the progression of moments, internal forces and displacements, from the
323 results obtained from the first. From the bending moment and the axial force values, it is then
324 possible to determine the safety factor along the perimeter of the lining and the minimum
325 value of the safety factor, representative for the entire support. This safety factor is then
326 plotted over time in order to evaluate the stability conditions of the lining during the tunnel
327 construction.

328 Subsequently, a parametric analysis was presented analyzing the behavior of the support in
329 two different types of rock mass types, considering two ARs of the excavation face and three
330 types of SC, with different curing rates. The study revealed that, generally, the minimum
331 safety factor is reached in the long term, when the curing of the SC is completed. However,
332 there are circumstances that produce a minimum of the safety factor in the transitory
333 conditions, after a few hours from the lining installation. In these circumstances, the major
334 problems with the stability of the lining are in the short term, rather than in the long term. This

335 can happen above all in the medium-high geomechanical rock types, in the presence of SC
336 with relatively slow curing, with high ARs.

337 **References**

- 338 1. Aydan, O., Sezaki M. and Kawamoto T. (1992). "Mechanical and numerical modelling
339 of shotcrete," in Pande, G., Pietruszczack, S. (Eds.), Numerical Models in
340 Geomechanics, Taylor and Francis, London, pp. 707-7016.
- 341 2. Bieniawski, Z. T. (1978). "Determining rock mass deformability". Int. J. Rock Mech.
342 Min.Sci., 15, 335–343.
- 343 3. Bryne, L. E. (2014). "Time Dependent Material Properties of Shotcrete for Hard Rock
344 Tunneling." Ph.D Thesis, Stockholm, Sweden.
- 345 4. Clements, M. (2004). "Comparison of methods for early age strength testing of
346 sprayed fibre reinforced concrete." In: Bernard, E.S. (Ed.), Proceedings of the 2nd
347 International Conference on Engineering Developments in Sprayed Fibre Reinforced
348 Concrete, Cairns, Queensland, Australia. Taylor and Francis Group, London, pp. 81–
349 87.
- 350 5. Chen, W.F. (1982). Plasticity in Reinforced Concrete. McGraw-Hill, New York.
- 351 6. Chang, Y., and Stille, H. (1993). "Influence of early age properties of shotcrete on
352 tunnel construction sequences." in Wood, D.F., Morgan, D.R. (Eds.), Shotcrete for
353 Underground Support VI, American Society of Civil Engineers, Reston, pp. 110-117.
- 354 7. Chang, Y. (1994). "Tunnel support with shotcrete in weak rock- A rock mechanics
355 study." Ph.D. Thesis, Division of Soil and Rock Mechanics, Royal Institute of
356 Technology, Stockholm, Sweden.
- 357 8. Concrete Institute of Australia (2010). Shotcrete in Australia. Concrete Institute of
358 Australia, Rhodes, Australia.
- 359 9. De Belie, N., Grosse, C.U., Kurz, J., and Reinhardt, H.W. (2005). "Ultrasound
360 monitoring of the influence of different accelerating admixtures and cement types for

- 361 shotcrete on setting and hardening behavior.” *Cement Concrete Res.*, 35, 2087 –
362 2094.
- 363 10. DIN (2014). *Spritzbeton - Nationale Anwendungsregeln zur Reihe DIN EN 14487 und*
364 *Regeln für die Bemessung von Spritzbetonkonstruktionen*, Beuth Verlag GmbH,
365 Berlin (in German).
- 366 11. DiNoia, T.P., and Sandberg, P.J. (2004). Alkali-free shotcrete accelerator interactions
367 with cement and admixtures. 2nd International Conference on Engineering
368 Developments in Shotcrete, pp. 137-144, A.A. Balkema Publishers, Leiden, London.
- 369 12. Do, N.A., Dias, D., Oreste, P., and Djeran-Maigre, I. (2014a). “A new numerical
370 approach to the hyperstatic reaction method for segmental tunnel linings.” *Int. J.*
371 *Numer. Anal. Meth. Geomech.*, 38, 1617–1632.
- 372 13. Do, N.A., Dias, D., Oreste, P., and Djeran-Maigre, I., (2014b). “The behavior of the
373 segmental tunnel lining studied by the hyperstatic reaction method.” *Eur. J.*
374 *Environmental Civil Eng.* 18(4), 489–510.
- 375 14. Fahimifar, A. and Hedayat, A. (2008). “Determination of ground response curve of the
376 supported tunnel considering progressive hardening of shotcrete lining.” *Proceedings*
377 *of the 5th Asian Rock Mechanics Symposium*, Tehran, Iran, November 24-26.
- 378 15. Fahimifar, A. and Hedayat, A. (2010). “Elasto-plastic analysis in conventional
379 tunnelling excavation.” *Proc. Inst. Civ. Eng. Geotech. Eng.*, 163(1), 37-45, doi:
380 10.1680/geng.2010.163.1.37.
- 381 16. Feenstra, P.H., and de Borst, B. (1993). “Aspects of robust computational models for
382 plain and reinforced concrete,” *Heron* 48(4), 5-73.
- 383 17. Graziani, A., Boldini, D., and Ribacchi, R. (2005). “Practical estimate of deformations
384 and stress relief factors for deep tunnels supported by shotcrete.” *Rock Mech. Rock*
385 *Engng.* 38 (5), 345–372.
- 386 18. Hellmich, C., Ulm, F.J. and Mang, H.A. (1999). „Multisurface chemoplasticity II:
387 numerical studies on NATM-tunneling.” *J Eng. Mech.-ASCE*, 125(6): 702-714.

- 388 19. Iwaki, K., Hirama, A., Mitani, K., Kaise, S., Nakagawa, K. (2001). „A quality control
389 method for shotcrete strength by pneumatic pin penetration test.” NDT and E
390 International, 34(6), 395-402.
- 391 20. Kotsovos, M.D. and Newman, J.B. (1978). “Generalized stress-strain relation for
392 concrete,” J. Eng. Mech.-ASCE, 104: 845-856.
- 393 21. Melbye, T. (1994). Sprayed Concrete for Rock Support. MBT International
394 Underground Construction Group, Zürich.
- 395 22. Meschke, G. (1996). “Elasto-viskoplastische Stoffmodelle für numerische
396 Simulationen mittels der Methode der Finiten Elemente,” Habilitationsschrift, TU
397 Wien.
- 398 23. Mohajerani, A., Rodrigues, D., Ricciuti, C., and Wilson, C. (2015). Early-Age Strength
399 Measurement of Shotcrete. Journal of Materials, ID 470160,
400 <http://dx.doi.org/10.1155/2015/470160>.
- 401 24. Moussa, A.M. (1993). Finite element modelling of shotcrete in tunnelling. PhD thesis,
402 University of Innsbruck, Austria.
- 403 25. Neuner, M., Schreter, M., Unteregger, D., and Hofstetter, G. (2017). “Influence of the
404 Constitutive Model for Shotcrete on the Predicted Structural Behavior of the Shotcrete
405 Shell of a Deep Tunnel.” Materials, 10, 577, doi:10.3390/ma10060577.
- 406 26. Neville, A.M., Dilger, W.H., and Brooks, J.J. (1983). Creep of Plain and Structural
407 Concrete. Construction Press, Harlow.
- 408 27. Oreste, P. (2003). “Procedure for Determining the Reaction Curve of Shotcrete Lining
409 Considering Transient Conditions.” Rock Mech. Rock Eng., 36(3), 209–236, DOI
410 10.1007/s00603-002-0043-z.
- 411 28. Oreste, P. (2007). “A numerical approach to the hyperstatic reaction method for the
412 dimensioning of tunnel supports.” Tunn. Undergr. Sp. Tech., 22:185–205.
- 413 29. Oreste P. (2009). “The Convergence-Confinement Method: Roles and limits in
414 modern geomechanical tunnel design.” American Journal of Applied Sciences 6(4),
415 757-771.

- 416 30. Oreste P. (2014). "The Determination of the tunnel structure loads through the
417 analysis of the Interaction between the void and the support using the convergence-
418 confinement method." *F American Journal of Applied Sciences*, 11(11), 1945-1954.
- 419 31. Oreste, P., Spagnoli, G., Luna Ramos, C.A., and Seville, L. (2018). "The Hyperstatic
420 Reaction Method for the Analysis of the Sprayed Concrete Linings Behavior in
421 Tunneling." *Geotech. Geol. Eng.*, <https://doi.org/10.1007/s10706-018-0454-6>.
- 422 32. Oreste, P., Spagnoli, G., and Luna Ramos, C.A., (2018b). "The Elastic Modulus
423 Variation During the Shotcrete Curing Jointly Investigated by the Convergence-
424 Confinement and the Hyperstatic Reaction Methods." *Geotech. Geol. Eng.*,
425 <https://doi.org/10.1007/s10706-018-0698-1>.
- 426 33. Pan, Y.W., and Huang, Z.L. (1994). "A model for the time dependent interaction
427 between rock and shotcrete support in a tunnel." *Int. J. Rock Mech. Min. Sci.* 31(3),
428 213-219.
- 429 34. Pöttler, R. (1990). "Time-dependent rock—Shotcrete interaction a numerical
430 shortcut." *Comp. Geotech.*, 9(3), 149-169.
- 431 35. prEN 934-5 (2003) *Admixtures for Concrete, Mortar and Grout—Part 5: Admixtures*
432 *for Sprayed Concrete—Definitions, Requirements and Conformity*.
- 433 36. Prudencio, L.R. Jr (1998). "Accelerating admixture for shotcrete." *Cem. Concr.*
434 *Compos.*, 20, 213–219.
- 435 37. Qiu, Y., Ding, B., Gan, J., Guo, Z., Zheng, C., Jiang, H. (2017). "Mechanism and
436 preparation of liquid alkali-free liquid setting accelerator for shotcrete". *IOP Conf. Ser.*
437 *Mater. Sci. Eng.*, 182, 012034, doi:10.1088/1757-899X/182/1/012034.
- 438 38. Rispin, M., Howard, D., Kleven, O. B., Garshol, K., Gelson, J. (2009). "Safer, Deeper,
439 Faster: Sprayed Concrete—An Integral Component of Development Mining,"
440 *Australian Centre for Geomechanics*.
- 441 39. Rokhar, R.B., and Zachow, R. (1997). "Ein neues Verfahren zur taglichen Kontrolle
442 der Auslastung einer Spritzbetonschale," *Felsbau* 15(6), 430-434.

- 443 40. Schädlich, B. and Schweiger, H.F. (2014). "A new constitutive model for shotcrete,"
444 in: Hicks, M.A., Brinkgreve, R.B.J., Rohe, A. (Eds.), Numerical Methods in
445 Geotechnical Engineering. Taylor & Francis, Oxam, pp. 103-108.
- 446 41. Schütz, R. (2010). "Numerical modelling of shotcrete for tunneling" Ph.D Thesis,
447 Imperial College London, UK.
- 448 42. Schütz, R., Potts, D.M., and Zdravkovic, L. (2011). "Advanced constitutive modelling
449 of shotcrete: Model formulation and calibration." *Comput. Geotech.* 38(6):834–845.
- 450 43. Spagnoli, G., Oreste, P., and Lo Bianco, L. (2016). "New Equations for Estimating
451 Radial Loads on Deep Shaft Linings in Weak Rocks." *Int. J. Geomech.*, 16(6),
452 06016006, [https://doi.org/10.1061/\(ASCE\)GM.1943-5622.0000657](https://doi.org/10.1061/(ASCE)GM.1943-5622.0000657).
- 453 44. Spagnoli, G., Oreste, P., and Lo Bianco, L. (2017). "Estimation of Shaft Radial
454 Displacement beyond the Excavation Bottom before Installation of Permanent Lining
455 in Nondilatant Weak Rocks with a Novel Formulation." *Int. J. Geomech.*, 17(9),
456 04017051 [https://doi.org/10.1061/\(ASCE\)GM.1943-5622.0000949](https://doi.org/10.1061/(ASCE)GM.1943-5622.0000949).
- 457 45. Thomas, A. (2009) *Sprayed concrete lined tunnels*. Taylor & Francis, Oxon.
- 458 46. Weber, J. W. (1979). "Empirische Formeln zur Beschreibung der
459 Festigkeitsentwicklung und der Entwicklung des E-moduls von Beton." *Betonwerk-*
460 *und-Fertigteilechnik*, 753–759.
- 461

462 **Figure caption**

463 **Fig. 1 Sprayed concrete trials in a job site.**

464 **Fig. 2 Trend of the elastic modulus over time for the three SC types considered in the**
465 **numerical example: SC_A: SC with fast curing rate ($\alpha=0.09$); SC_B: SC with medium**
466 **curing rate ($\alpha=0.05$) and SC_C: SC with low curing rate ($\alpha=0.03$).**

467 **Fig. 3 Trend of UCS over time for the three SC types considered in the numerical**
468 **example: SC_A: SC with fast curing rate ($\alpha=0.09$); SC_B: SC with medium curing rate**
469 **($\alpha=0.05$) and SC_C: SC with low curing rate ($\alpha=0.03$).**

470 **Fig. 4 Rock type 1: Evaluation of FS over time for the three SC types (SC_A ($\alpha=0.09$), SC_B**
471 **($\alpha=0.05$) and SC_C ($\alpha=0.03$)) and two advance rates.**

472 **Fig. 5 Rock type 2: Evaluation of FS over time for the three SC types (SC_A ($\alpha=0.09$), SC_B**
473 **($\alpha=0.05$) and SC_C ($\alpha=0.03$)) and two advance rates.**

474

475 **Table caption**

476 **Table 1. Mechanical characteristics of the rock type 1 (RMR = 60), considered in the**
477 **studied example.**

478 **Table 2. Mechanical characteristics of the rock type 2 (RMR = 80), considered in the**
479 **studied example.**